Glass states and freezing transition in (NH4I)x(KI)1−x

M. Winterlich, R. Böhmer, Alois Loidl

Angaben zur Veröffentlichung / Publication details:

Winterlich, M., R. Böhmer, and Alois Loidl. 1995. "Glass states and freezing transition in (NH4I)x(KI)1−x." *Physical Review Letters* 75 (9): 1783–86. https://doi.org/10.1103/physrevlett.75.1783.

Glass States and Freezing Transition in $(NH_4I)_x(KI)_{1-x}$

M. Winterlich, R. Böhmer,* and A. Loidl

Institut für Festkörperphysik, Technische Hochschule Darmstadt, D-64289 Darmstadt, Germany

(Received 10 April 1995)

The glass transition in $(NH_4I)_x(KI)_{1-x}$ has been studied using dielectric spectroscopy. The (x,T) phase diagram reveals three different glassy regions, g_1, g_2, and g_3. The dynamical susceptibility in the regime g_2 reveals a power-law dependence on frequency, $\epsilon^* \propto A(T)\omega^{s(T)}$. The experimental results are compared with theoretical models and provide evidence for the near-equilibrium dynamics in an orientational glass.

PACS numbers: 64.70.Pf, 77.22.Ch

The nature of the freezing transition in disordered systems is still an unsolved problem. Early theories based on Ising-type mean field (MF) models for spin glasses [1,2] predicted sharp transitions. Within the infinite-range model of Sherrington and Kirkpatrick (SK) [2], the Almeida-Thouless (AT) line [3], separating paramagnetic, ferromagnetic, and glass phases, has been calculated. Below the AT line the system becomes nonergodic. A series of experimental results indicated the existence of the AT line in some spin glasses (SG's). However, it was shown later that at least part of the data can also be explained by a zero-temperature transition [4]. Sompolinsky and Zippelius (SZ) [5] have investigated dynamic properties of the SK model above and below the AT line introducing a soft-spin version for Ising spins. Later on, Fischer and Kinzel [6] extended this analysis to a larger range of frequencies, temperatures, and fields. Concerning the imaginary part of the dynamical susceptibility χ'', this MF theory yields the following predictions: (i) a sharp increase for small frequencies and fields near the AT line, (ii) a frequency dependence $\chi'' \propto \omega^s$, with a frequency exponent $s = 0.5$ at the freezing transition and $s \sim 0.25-0.4$ for $T \rightarrow 0$ K and zero fields, and (iii) $\chi'' \propto T$ at low temperatures and for all fields.

Of course, MF theory does not seem to be adequate to describe the relaxation dynamics below the freezing temperature $T_f(\omega)$. Hence Fisher and Huse (FH) [7,8] worked out a phenomenological scaling approach to the static and dynamic properties of finite-range SG's. In this picture of the ordered SG phase, the low-lying excitations which dominate the correlations are droplets of coherently flipping spins. According to this scaling approach $\chi'' \propto (\ln\omega\tau_c)^{-(1+\beta)}$. Here τ_c is a microscopic time ($\sim 10^{-12}$ s) and the exponent $\beta \sim 1$, for the most naive assumptions for three-dimensional systems [7].

In the analysis of the experimental results most SG's [9] have been characterized by the frequency dependence of the freezing temperature T_f. However, $T_f(\omega)$ usually is determined from the cusp in the temperature dependence of the real part of the dynamic magnetic susceptibility $\chi'(\omega,T)$ only. Measurements of the absorption are scarce, and for most of these results little can be said with respect to the models outlined above. Among the few exceptions are reports concerning measurements of the dynamical susceptibility in the insulating SG (Eu,Sr)S [10,11]. The most convincing experimental evidence for a power-law dependence of $\chi''(\omega)$ has been given for $Eu_{0.4}Sr_{0.6}S$ [11]. These results have been interpreted in terms of a true phase transition into a disordered ground state.

Orientational glasses (OG's) [12] are the molecular analogs of SG's. In dipolar systems the dielectric permittivity $\epsilon^* = \chi^* + 1$ has been studied in full detail, covering broad frequency and temperature ranges. The majority of these systems reveal an Arrhenius-type slowing down of the mean relaxation rates, which is convincingly documented in the frequency dependence of the complex dielectric constant $\epsilon^*(\omega) = \epsilon_1(\omega) - i\epsilon_2(\omega)$ for a large variety of materials [12]. In addition, dipolar glasses reveal broad and almost symmetric loss peaks and a striking increase of the distribution of relaxation times with decreasing temperatures [12,13]. Partly, this behavior can be explained by a Gaussian distribution of energy barriers, introduced by random fields which are created by substitutional defects [13]. The cooperativity of the freezing transition usually is inferred from the concentration dependence of the freezing temperature T_f or from slight deviations from the Arrhenius behavior of the mean relaxation rates [12]. In analogy to magnetic systems, the AT line has been determined via the splitting between field-cooled and zero-field-cooled dipolar susceptibilities [14] or via a divergence of the nonlinear (third-order) susceptibility [12,15]. However, the transition temperatures determined by these experiments are still frequency dependent, and one has to be cautious when conclusions concerning a static freezing temperature are drawn. To solve this problem, recently a new frequency-temperature plot of the dielectric constant has been proposed to determine the divergence of the low-frequency edge of the dielectric relaxation [16].

The observation of a power-law behavior of the imaginary part of the dielectric constant $\epsilon_2 \propto \omega^s$, indicative of a glassy relaxational dynamics, has been detected in the dipolar glass system $K_{1-x}Na_xTaO_3$ [15] only. The parameter s (frequency exponent) was small ($s < 0.1$) and frequency independent. In this Letter we present dielectric results on the OG $(NH_4I)_x(KI)_{1-x}$. Previously [17],

we tried to describe the dielectric data for $x = 0.43$ by an unusual broad distribution of relaxation times. Here we present detailed and systematic investigations which shows that the complex dielectric permittivity in this system can well be described by a power-law behavior. Our experimental results provide experimental evidence for the near-equilibrium dynamics of a molecular system in its glassy phase and can be used to test theoretical predictions.

Gold-plated crystals $(NH_4I)_x(KI)_{1-x}$ with concentrations $0.1 < x < 0.8$ have been investigated. All crystals were grown from an aqueous solution. The NH_4I concentration x was determined using the concentration dependence of the lattice constants [18]. Measurements of the dielectric constant ϵ_1 and the dielectric loss ϵ_2 were performed at frequencies $10^2 \leq \nu \leq 10^9$ Hz and temperatures $1.5 \leq T \leq 300$ K.

Figure 1 shows the temperature dependence of the dielectric constant ϵ_1 (upper frame) and of the dielectric loss ϵ_2 (lower frame) at a measuring frequency of 100 kHz, for different concentrations in $(NH_4I)_x(KI)_{1-x}$. With decreasing temperatures and for all concentrations investigated, $\epsilon_1(T)$ reveals a Curie-Weiss-like increase, passes through a cusp-shaped maximum, and finally decreases towards low temperatures. The temperature of the cusp maximum $T_m(x)$ exhibits a pronounced concentration dependence, a behavior that directly evidences that the freezing is interaction dominated. The loss phenomena (Fig. 1, lower frame) are small, and the temperature of the loss maxima as well as the shape of the loss curves strongly depend on the concentration. For example, a single loss peak appears for concentrations $x \leq 0.45$, while double peak structures develop for higher x. The anomaly at higher temperatures corresponds to a transition into a short-range ordered ϵ phase. The second anomaly presumably indicates a freezing transition of the rotational degrees of freedom only [18]. For $x \geq 0.55$ the loss phenomena become very small.

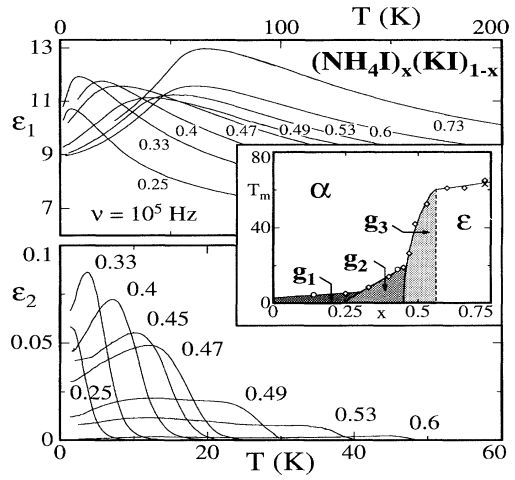

FIG. 1. Temperature dependence of the dielectric constant ϵ_1 (upper frame) and of the dielectric loss ϵ_2 (lower frame) as measured at 100 kHz in $(NH_4I)_x(KI)_{1-x}$ for concentrations $x = 0.25$, 0.33, 0.4, 0.45, 0.47, 0.49, 0.53, 0.6, and 0.73. The inset shows the concentration dependence of the temperature of the peak maximum (T_m) of the real part of the dielectric constant. Besides the paraelectric α phase and the orientationally ordered ϵ phase, three different glassy regimes, g_1, g_2, and g_3, show up.

For a closer inspection $T_m(x)$ is plotted in the inset of Fig. 1. $T_m(x)$ depends weakly on x for NH_4I concentrations $x > 0.55$, but rapidly decreases in the range $0.45 < x < 0.55$, followed by a linear decrease, and finally by a smooth tailing off towards the lowest concentrations. From neutron scattering investigations [18,19] we know that at concentrations $0.55 < x < 0.8$ $(NH_4I)_x(KI)_{1-x}$ exhibits the trigonal ϵ phase in which the ammonium ions occupy two independent lattice sites and reveal a complex orientational order [19]. For $0.45 < x < 0.55$ the structure remains cubic with short-range structural and orientational orders reminiscent of the ϵ phase. This has been deduced from x-ray [20] and neutron scattering experiments [18] and has been detected for the first time in deuterated compounds by Berret *et al.* [21]. In deuterated compounds two anomalies have been detected by nuclear magnetic resonance experiments [22], in accordance with the double peak structure in $\epsilon_2(T)$ in the protonated compounds for $x > 0.45$ (see Fig. 1) [23]. Finally, below concentrations $x = 0.45$ the NH_4 ions freeze in randomly in a cubic fcc lattice.

The (x, T) phase diagram (inset of Fig. 1) reveals three distinct disordered low-temperature regimes, g_1, g_2, and g_3. For concentrations $0.45 < x < 0.55$ (g_3, light-shaded area), local ϵ-like distortions dominate. As discussed above, the loss in g_3 is small and exhibits a double peak structure. For $0.25 \leq x \leq 0.45$ (g_2, shaded area), well defined loss peaks exist. The transition line from the paraelectric high-temperature α phase to the glass state g_2 decreases linearly towards $x = 0.2$, which is the percolation limit of the fcc lattice. This behavior implies that the transition into the disordered state g_2 is dominated by next-nearest-neighbor interactions. Finally, for $x < 0.25$, $T_m(x)$ depends only weakly on temperature. Hence we conclude that the glassy regime g_1 (dark-shaded area) is dominated by relaxations of single NH_4 ions only weakly disturbed by dipolar interactions. The disordered state g_1 is the regime in which the ammonium ions slow down in the Born-Mayer potential set by the neighboring ions.

In what follows we will take a closer look at the glassy regime g_2 which reveals, when compared to other dipolar glasses, very unusual dielectric features. The power-law behavior of the dielectric permittivity reveals that true equilibrium behavior can only be reached asymptotically.

Figure 2 shows the dispersive region of $\epsilon_1(T)$ (upper frame) and $\epsilon_2(T)$ (lower frame) in $(NH_4I)_{0.33}(KI)_{0.67}$ at three different measuring frequencies. The data reveal a striking similarity with the complex magnetic susceptibility in the insulating spin glass $Eu_{0.4}Sr_{0.6}S$ [11].

In Fig. 3 the frequency dependence of ϵ_2 is shown as $\log_{10}(\epsilon)$ vs $\log_{10}(\nu)$ for $x = 0.25$. Despite the fact that,

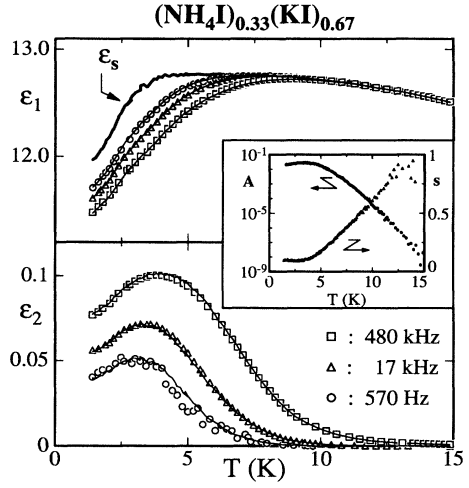

FIG. 2. Real part (upper frame) and imaginary part (lower frame) of the dielectric constant in $(NH_4I)_{0.33}(KI)_{0.67}$ at three probing frequencies: 480 (□), 17 (△), and 0.57 kHz (○). The solid lines are calculated as described in the text. The thick solid line represents the theoretically extrapolated static susceptibility. The inset shows the fit parameters A and s for this concentration.

due to the low losses of the material, the data points reveal large uncertainties at radio frequencies, a power-law behavior is obeyed over six decades in frequency. Any description of these data in terms of a distribution of relaxation times needs a distribution function $g(\tau)$ covering at least 20 decades. The inset shows the frequency dependent data for $x = 0.33$ at audio frequencies. It is important to note that the data reveal no significant curvature in the log-log representations of Fig. 3.

In the introduction we mentioned two models for the description of the relaxation dynamics below the freezing temperature. In the SZ model [5] the dissipative part of the susceptibility should obey a power law $\chi'' = A\omega^s$, with s of order 0.5. In the droplet model of FH [7,8] s should be roughly constant over wide ranges of frequency, but with a slight curvature according to $s \sim (1 + \beta)/|\ln\omega\tau_c|$. Assuming $\beta \sim 1$ and $\tau_c \sim 10^{-12}$ s [7], the exponent should change from $s \sim 0.1$ at 1 kHz to $s \sim 0.29$ at 1 GHz. Our experimental results reveal a constant slope for all concentrations and temperatures investigated. Hence we parametrized our data with a pure power-law dependence on frequency, with parameter s depending on temperature only.

Accordingly, the complex dielectric constant can be described using $\epsilon^* = \epsilon_s - \frac{2}{\pi}\frac{A(T)}{s(T)}\omega^{s(T)} + iA(T)\omega^{s(T)}$. Here ϵ_s is the static dielectric constant, and the real and imaginary parts are strictly related via the Kramers-Kronig transformation. The solid lines in Figs. 2 and 3 through the data points represent the results of fits of this model to the experimental data, using the parameters $A(T)$, $s(T)$, and ϵ_s. ϵ_s is indicated as a thick solid line in the upper frame of Fig. 2. Following these lines we parametrized the experimental results for all concentrations in the glass regime g_2. The temperature dependence of the parameters A and s, for all $(NH_4I)_x(KI)_{1-x}$ crystals investigated, is presented in Fig. 4. $A(T)$ reveals a cusplike maximum. The maximum value of A, for a given concentration, closely corresponds to the maximum in $\epsilon_2(T)$, which indicates the freezing temperature T_g. On the high-temperature side A steadily decreases. The frequency exponent s decreases with decreasing temperatures and yields a limiting low-temperature value $s \sim 0.07$. For all x, this limiting value of s is reached at the cusp maximum of $A(T)$. This means that below the freezing transition the apparent frequency exponents are in reasonable agreement with the predictions of the FH droplet model in the audiofrequency range, but are much smaller than those of order 0.5 for the SZ model. However, in contradiction

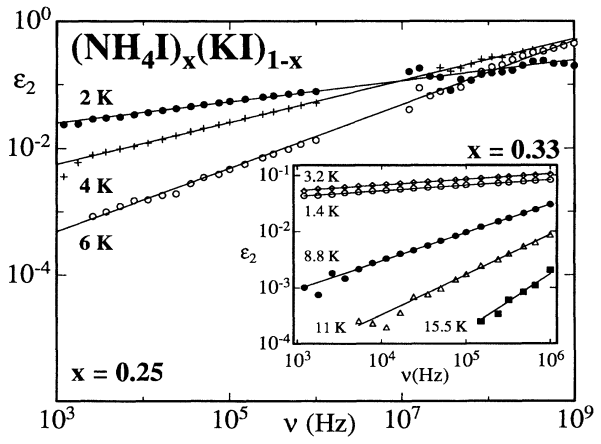

FIG. 3. $\log_{10}\epsilon_2$ vs $\log_{10}\nu$ in $(NH_4I)_{0.25}(KI)_{0.75}$. The solid lines represent power laws, according to $\epsilon_2 = A\omega^s$. The inset shows similar results for $(NH_4I)_{0.33}(KI)_{0.67}$ obtained in the audiofrequency range.

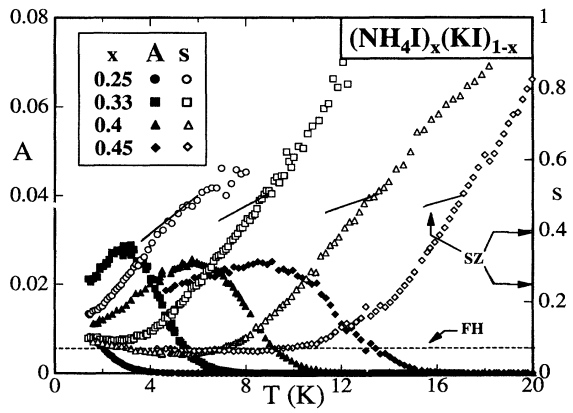

FIG. 4. Temperature dependence of the parameters A (solid symbols) and s (open symbols), as determined in $(NH_4I)_x(KI)_{1-x}$ for concentrations $x = 0.25$, 0.33, 0.4, and 0.45. The solid lines indicate the predictions of the SZ model at $T \leq T_f$. The arrows indicate the limiting zero-temperature results. The dashed line is the FH result as explained in the text.

to the FH model, we find no experimental evidence of frequency dependent exponents s.

The parameters A and s develop continuously with decreasing temperatures. This behavior is clearly demonstrated for $x = 0.33$ by the inset of Fig. 2 in which $\log_{10} A$ is plotted vs temperature. From the highest temperature, where loss phenomena can be detected, s decreases from values close to 1 and A increases smoothly over many orders of magnitude. The value of $s = 0.5$, as predicted in the SZ model at T_f, obviously is reached far above T_f. The SZ predictions for $s(T \lesssim T_f) = \frac{1}{2} - \frac{1}{\pi}(T_f - T)/T_f$ are indicated in Fig. 4 by solid lines, the predictions for $s(T = 0)$ by arrows.

Finally, we would like to comment on the freezing dynamics. As can be seen in Fig. 2, the peak maximum in $\epsilon''(T)$ slightly shifts towards lower temperatures with decreasing frequencies. Defining the frequency of the peak maximum as the characteristic relaxation rate, the slowing down of these rates follows an Arrhenius law $\nu = \nu_0 \exp(-E_B/k_B T)$ for all concentrations. The energy barriers are of order 10 K for $x \leq 0.25$ but increase strongly towards higher concentrations, reaching $E_B \sim 350$ K at $x = 0.45$. The attempt frequencies ν_0 reveal realistic microscopic times only for $x \leq 0.25$, e.g., $\nu_0 = 8.8 \times 10^{10}\ \mathrm{s}^{-1}$ for $x = 0.25$. They reach values of order $10^{20}\ \mathrm{s}^{-1}$ for the higher concentrations, showing that a parametrization in terms of an activated behavior is not meaningful. This again demonstrates unambiguously that the relaxation dynamics for $x < 0.25$ is due to thermally activated reorientations of isolated ammonium molecules, while the relaxational behavior in the glass regime g_2 is characteristic for the near-equlibrium dynamics of a glass phase.

This work was supported by the Deutsche Forschungsgemeinschaft via the SFB 262. We thank A. Maiazza for growing the high-quality single crystals used in this work.

*Present address: Institut für Physikalische Chemie, Johannes Gutenberg-Universität, D-55099 Mainz, Germany.

[1] S. F. Edwards and P. W. Anderson, J. Phys. F **5**, 965 (1975).
[2] D. S. Sherrington and S. Kirkpatrick, Phys. Rev. Lett. **35**, 1792 (1975).
[3] J. R. L. de Almeida and D. J. Thouless, J. Phys. A **11**, 983 (1978).
[4] K. Binder and A. P. Young, Phys. Rev. B **29**, 2864 (1984).
[5] H. Sompolinsky and A. Zippelius, Phys. Rev. B **25**, 6860 (1982).
[6] K. A. Fischer and W. Kinzel, J. Phys. C **17**, 4479 (1984).
[7] D. S. Fisher and D. A. Huse, Phys. Rev. B **38**, 373 (1988).
[8] D. S. Fisher and D. A. Huse, Phys. Rev. B **38**, 386 (1988).
[9] K. Binder and A. P. Young, Rev. Mod. Phys. **58**, 801 (1986).
[10] D. Hüser, L. E. Wenger, A. J. van Duyneveldt, and J. A. Mydosh, Phys. Rev. B **27**, 3100 (1983).
[11] C. C. Paulsen, S. J. Williamson, and H. Maletta, Phys. Rev. Lett. **59**, 128 (1987).
[12] U. T. Höchli, K. Knorr, A. Loidl, Adv. Phys. **39**, 405 (1990).
[13] A. Loidl and R. Böhmer, in *Disorder Effects on Relaxational Processes,* edited by R. Richert and A. Blumen (Springer-Verlag, Berlin, 1994), p. 659.
[14] A. Levstik, C. Filipic, Z. Kutnjak, I. Levstik, R. Pirc, B. Tadic, and R. Blinc, Phys. Rev. Lett. **66**, 2368 (1991).
[15] M. Maglione, U. T. Höchli, and J. Joffrin, Phys. Rev. Lett. **57**, 436 (1986).
[16] Z. Kutnjak, C. Filipic, A. Levstik, and R. Pirc, Phys. Rev. Lett. **70**, 4015 (1993).
[17] I. Fehst, R. Böhmer, W. Ott, A. Loidl, S. Haussühl, and C. Bostoen, Phys. Rev. Lett. **64**, 3139 (1990).
[18] M. Paasch, M. Winterlich, R. Böhmer, R. Sonntag, G. J. McIntyre, and A. Loidl, Z. Phys. B (to be published).
[19] M. Paasch, G. J. McIntyre, M. Reehuis, R. Sonntag, and A. Loidl, Z. Phys. B (to be published).
[20] T. Umeki, K. Yagi, and H. Terauchi, J. Phys. Soc. Jpn. **63**, 876 (1994).
[21] J. F. Berret, C. Bostoen, J.-L. Sauvajol, B. Hennion, and S. Haussühl, Europhys. Lett. **16**, 91 (1991).
[22] R. Böhmer, F. Fujara, and G. Hinze, Solid State. Commun. **86**, 183 (1993).
[23] From our present experience we suspect that deuteration introduces only minor changes in the (x, T) phase diagram. However, a detailed phase diagram has not been determined so far.